International Journal of Geography, Geology and Environment

**P-ISSN:** 2706-7483
**E-ISSN:** 2706-7491
IJGGE 2023; 5(2): 111-121
Received: 05-05-2023
Accepted: 13-06-2023

**Chibuogwu IU**
Nnamdi Azikiwe University, Awka, Anambra, Nigeria

**Ugwu GZ**
Enugu State University for Science and Technology, Enugu, Nigeria

**Corresponding Author:**
**Chibuogwu IU**
Nnamdi Azikiwe University, Awka, Anambra, Nigeria

# Examining tunnel erosion using vertical electrical sounding and ground magnetic geophysical techniques in Awka, Nigeria

**Chibuogwu IU and Ugwu GZ**

**DOI:** https://doi.org/10.22271/27067483.2023.v5.i2b.179

**Abstract**
The present study investigates the nature and characteristics of soil piping using Vertical Electrical Sounding (VES) and Magnetic geophysical techniques at Awka, Nigeria. The VES survey was conducted using a Pasi resistivity meter, while the ground magnetic survey was carried out using a proton precision magnetometer. The VES survey revealed two to five distinct geo-electrical sections and fourteen characteristically sounding curves, which indicate vertical changes in the subsurface. The findings illustrate that the weathered soil in proximity to the surface of the study area has the best soil formations that encourage soil pipe development. Moreover, the iso-resistivity 2D maps demonstrate that the soil pipes describe a direction in the NW-SE, which is consistent with the stress direction, fluid migration paths, and sloppy terrains of the study area. The results of the ground magnetic survey were obtained using a diurnal corrected anomaly technique generated from the field. This finding suggests that low magnetic susceptibility, ranging from -124.4 to -300nT, has accumulated in the subsurface, primarily in the south-western region, where most of the soil pipes are located in the surveyed areas.

**Keywords:** Tunnel erosion soil piping, soil subsidence, geophysical technique, VES, magnetic survey, diurnal, Awka

## Introduction
Piping is a phenomenon that occurs when water is eroded beneath the surface of the earth to create an underground tunnel known as a "soil pipe." This soil pipe, also known as tunnel erosion, usually starts as a tiny pore in the subsurface, and with time, it can grow large enough to form channels in which soil and other materials are transported, consequently leading to an increase in both subsurface erosion and surface erosion (Chibuogwu & Ugwu, 2023a; Joshi *et al*., 2021) [27, 13].

Soil piping occurs in many ways, the first and most common is during rainfall. Here, percolating water carrying fine silt and clay particles forms passageways that create conduits called "soil pipes," which are commonly a few millimeters to a few centimeters in size but can grow to a meter or more. They may lie very close to the surface or extend several meters below the ground. Once initiated, they become cumulative, and the conduits they form expand with respect to time. Further subsurface erosion of the conduit will lead to roof collapse and subsidence features on the surface. In many cases, the phenomenon goes unnoticed since it happens underground (Bernatek-Jakiel & Poesen, 2018; Bryan, 2000) [3, 6].

Secondly, soil pipes can be formed from openings in the ground that were left behind when a plant died or a tree was uprooted. Animals can also help to create soil pipes by burrowing and tunneling in the soil, humans can also excavate land during the construction of urban residences and during the period of road construction; many roads are poorly leveled, and with time, they tend to cave in, providing a process for soil pipe and tunnel erosion to build up. Another way in which humans contribute to the piping process is during mining, in search of precious materials, the ground is opened, and most of the time it is left in that state after the mining process is done. This action opens up the area for erosion and soil pipe to take place (Chibuogwu & Ugwu 2023a) [27].

The piping process involves a relatively weak incoherent layer that becomes saturated and conducts water on some surfaces. The free face could be the wall or head of a gully, the head cut off by a landslide, or a man-made excavation. The more flow it carries, the faster it will grow by enlarging its diameter and by headward sapping.

As the flow rates increase through the pipes, it further corrodes the conduit, resulting in the collapse of the walls and roof. The collapse of the wall and roof further produces a line of sinks, which then act as tunnels to convey surface runoff into other developing pipes. During this process, the weaker portions of the pipes will lose their grip on the surrounding structure and collapse, leaving an open gully or sinkhole (Land subsidence) (Atallah *et al*., 2015) [2].

The objective of this study was to examine the spatial distribution, pattern, and characteristics of soil pipes in an area renowned for tunneling erosion in Awka, Anambra State, Nigeria. To accomplish this objective, we utilized two geophysical techniques: vertical electrical sounding (VES) and ground magnetic techniques.

**Geology of the study area**

The location being studied is situated in the Anambra basin (figure 1), which forms part of the lower Benue trough tectonic unit. Various researchers, such as (Wright, 1968) [24], have conducted a detailed analysis of the regional stratigraphy and geology of the trough. The beginnings of the Anambra Basin can be traced back to the Santonian-Campaman periods, when there was a widespread tectonic shift in the area due to a tensional regime during the Cretaceous epoch. This geological event is responsible for the formation of the present-day Anambra Basin (Rayment, 1965) [22].

The basin's sediments were deposited during the Cretaceous period and had a directional orientation of NW-SE. The layers of these sediments gently slope toward the north. Awka town and its surrounding areas are primarily situated on the Imo shale. This shale has a fine texture and varies in shades from dark grey to bluish-grey, with some parts containing clay ironstone and sandstone bands, as shown in Figure 1. Towards the top, the Imo shale becomes sandier, and may contain alternating bands of sandstone and shale, according to (Agagu & Adighije, 1983) [1] analysis.

The soils found in Anambra State, specifically the coastal plain sands, play a significant role in the ecological challenges faced by the region. These soils exhibit high susceptibility to erosion and are characterized by the presence of groundwater reservoirs. Underlying these weak lateritic and acidic soils are geologic rocks and materials that are unstable and poorly consolidated. Of particular importance are the sandy members of these geologic units, which contain substantial groundwater reservoirs known as aquifers. The pore water pressures within these aquifers can pose a threat when subjected to excessive loads from overlying structures. Additionally, the lateritic and sandy soils are prone to erosion caused by storm water runoffs (Chibuogwu & Ugwu, 2023b) [8].

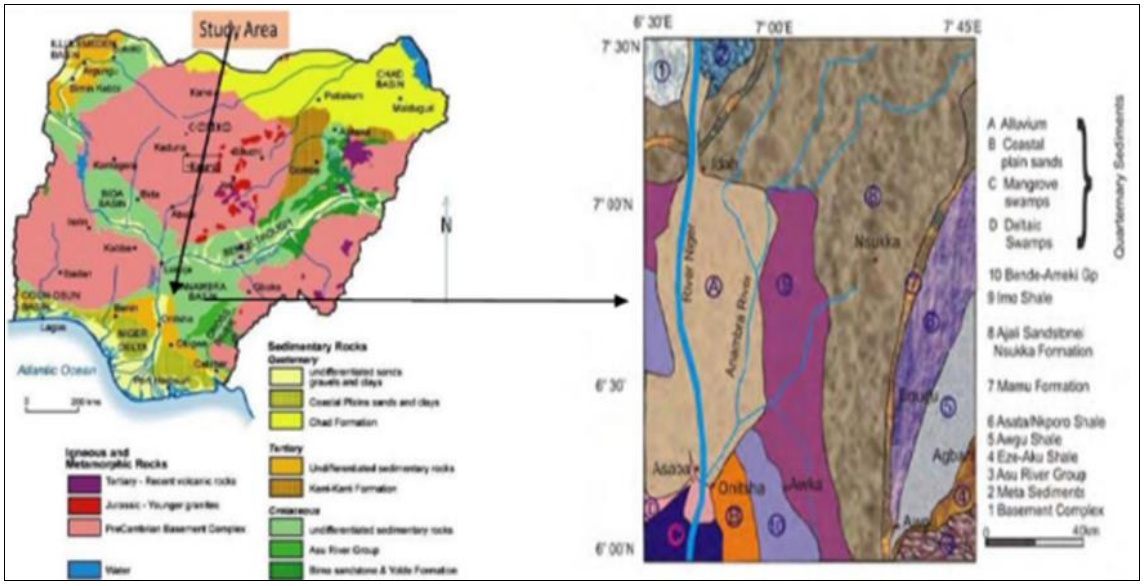


**Fig 1:** Map of the geological setting of Nigeria and Anambra Basin

**Study Area**

In this study, our focus is on two specific sites within the Awka South local government area of Anambra State, Nigeria (as shown in Figure 1). The first site, Awka Site 1, is situated at coordinates (6.2232°N and 7.0824°E). Here, a soil pipe with a diameter of approximately 5cm has caused significant damage to a constructed road. This damage has resulted in the formation of double sinkholes, each with a diameter of around 70cm (refer to Figure 2a).

The Awka Site 2, located at coordinates (6.222°N and 7.0819°E), we find a soil pipe that has been present for approximately three years. This pipe has caused the formation of multiple holes, each with an average diameter of 10 cm, as well as a visible sinkhole measuring around 100 cm in diameter (as depicted in Figure 2b).

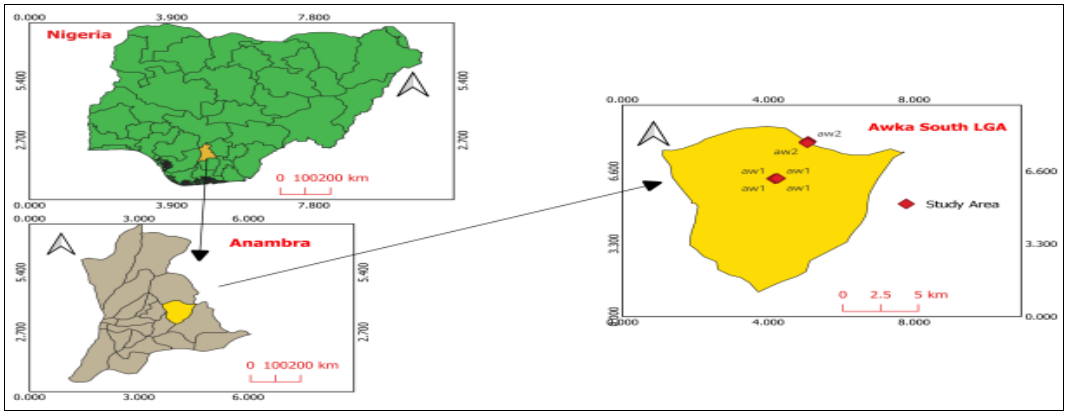


**Fig 2:** Map showing the surveyed state and LGA

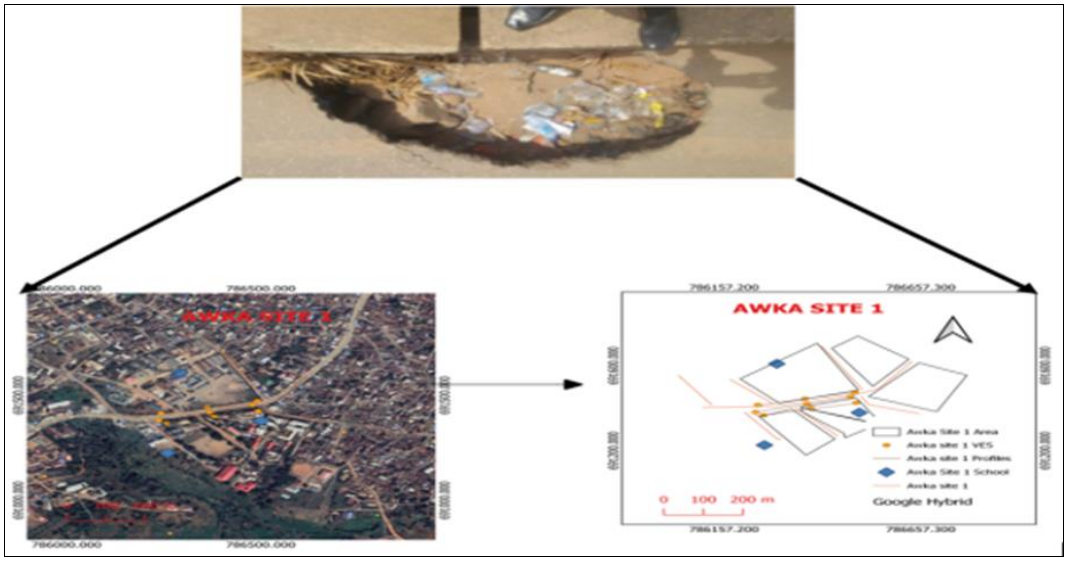


**Fig 3:** Map of soil pipe, satellite image and survey points in Awka site 1

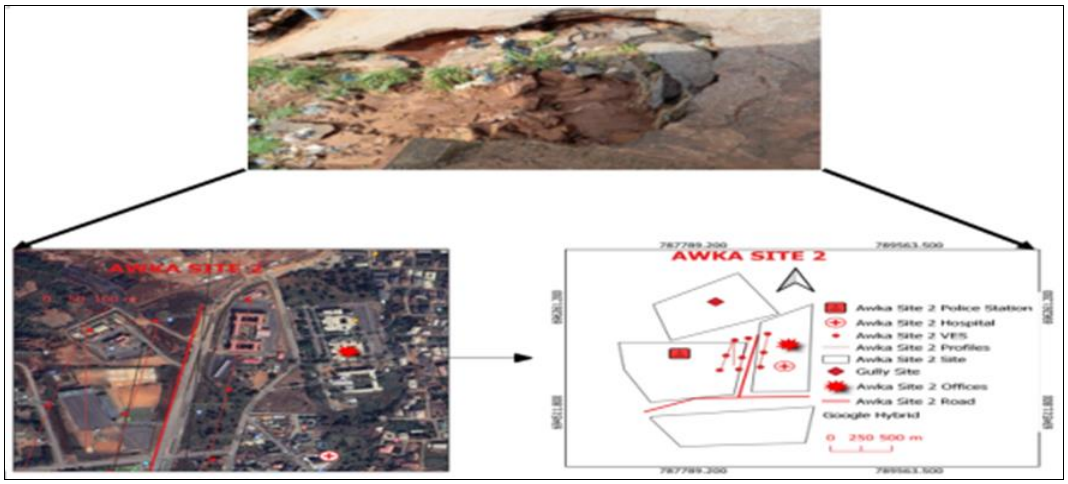


**Fig 4:** Map of soil pipe, satellite image and survey points in Awka site 1.

## Methods

### Vertical Electrical Sounding Method

The Vertical Electrical Sounding (VES) technique employed in this study utilized the Schlumberger electrical array (Olafisoye, 2013; Zohdy, 1974) [19, 24], with the apparent resistivity measured using the Pasi resistivity meter. A total of eighteen electrical soundings were conducted, as depicted in Figures 5 and 6. The maximum half current electrode spacing (AB/2) utilized was 100m. Subsequently, the field data underwent analysis by employing the partial curve matching technique (Gouet *et al*., 2020; Olafisoye, 2013) [12, 19]. For this study, we employed established matching techniques such as the use of master curves (Olafisoye, 2013) [19] and sets of auxiliary diagrams (Olafisoye, 2013; Zohdy, 1974) [19, 25] to derive initial estimations of the resistivity and thickness of the different geoelectric layers at each VES location. These estimations served as the initial models for subsequent computerized iterations, which were facilitated by the IpI2 win software.

By conducting a partial curve fitting analysis, we successfully derived a curve model that consisted of 3-5 layers (resistive-conductive-resistive) for the eighteen VES sites that were investigated. This model provides valuable insights into the geoelectric properties of the subsurface in these locations.

**Magnetic Method**

Portable proton precession type magnetometers and GPS navigation equipment were used to acquire the ground magnetic field data along 9 profiles with approximately 2m interspacing (as shown in Figures 3 and4). Each profile consisted of 20 moving stations at a minimum spacing of 1m, oriented in the North-South direction, to create a 2 m × 2 m grid. To ensure accuracy, a suitable base station was located in an area far from any magnetic substance in the study area. This base station recorded readings at 10-minute intervals to correct for diurnal variations, which were rectified by subtracting base values from measured grid values. The diurnal corrected data were gridded using the minimum curvature method and plotted using the Origin software package. However, the study did not consider the International Geomagnetic Reference Field (IGRF) and regional-residual separation due to limitations in the study area.

**Results**

**Result for Vertical Electrical Sounding**

When analyzing the Vertical Electrical Sounding (VES) survey data, the obtained VES curves were plotted in bi-logarithmic graphs, as illustrated in Figures 5 and 6. These graphs showcased the relationship between the field's apparent resistivity observations and the half-electrode spacing (AB/2) or depth below the subsurface. To interpret these curves, manual partial curve matching was employed, wherein the curves were compared with different master curves. Subsequently, the resulting curves in Figures 5 and 6 were digitally generated using the IPI2win computer software. These digitally generated curves were then compared to the manually generated curves to achieve optimal outcomes. The best-fit model for each sounding was utilized to ensure the lowest possible Root Mean Square (RMS) error. The theoretical curve for the best-fit model is represented by a solid line overlaying the observed curve. Additionally, the blue blocks depicted on the graph provide information regarding the true resistivity value (ρ), depth (e), and thickness (t) distribution of the geological layers.

The observed curves in the study profiles provide valuable insights into the horizontal and vertical variations of the layers. Tables 1 and 2 present the distribution of layers across different soundings. The curves are categorized into various types, namely H, K, KA, HA, HK, AK, HKQ, HKH, KHK, AKQ, and KHA, for both study areas. These curve types correspond to the distributed layers and offer a comprehensive description of the geoelectric properties. Due to the vertical electrical anisotropic properties of the study areas, these curves delineate two to five geoelectric layers.

In Awka site 1, the AK curve dominates, accounting for 33.3% of the frequency, whereas the HK, HKH, and KHK curves occur more than once for both sites, with a frequency of 22.2%. The remaining curves appear only once, representing 11.1% of the frequency. These frequency distributions provide valuable insights into the prevalence of different curve types and their significance in characterizing the geoelectric layers in the study areas.

The bi-logarithmic curves obtained from the graph, as shown in Figures 5 and 6, were utilized to generate the geo-electric sections. These sections provide a visual representation of the vertical variations in layers along each profile within the subsurface, reaching depths of approximately 84m for Awka site I and 35m for Awka site II. Through the analysis of these sections, it was possible to identify and delineate three to five distinct geo-electric layers, considering both the electrical characteristics of the subsurface (resistivity, ρ, thickness, t, and depth, e).

In particular, in Awka site I (Figure 9), the layer that prominently occurred was found to be the weathered decayed soil, exhibiting a resistivity range between $1200 < \rho < 30000\Omega m$. It is worth noting that within a depth range of $0 < e < 6m$, soil pipes or tunnels may form within this layer. This phenomenon can be attributed to the high resistivity at this depth, which encourages dispersion in the soil, subsequently leading to an increase in seepage pressure. This observation aligns with previous studies conducted by Bhagyalekshmi *et al*. (2015) [4], Joshi *et al*. (2021) [13], and Onda (1994) [20].

At the opposite end of the geo-electric section, we encounter a distinctive thin layered structure known as the conductive soil, exhibiting remarkably low resistivity values ranging from $10 < \rho < 100\Omega m$. This layer predominates in Awka site 2, as depicted in Figure 10. It is important to note that this conductive soil can be considered as contaminated topsoil since it occurs in close proximity to the surface of the profile, within the depth range of $0 < e < 2m$.

The presence of this conductive soil layer serves as a protective blanket, effectively preventing excessive seepage flow and thereby discouraging the formation of soil pipes. In addition to the conductive soil layer, other notable geo-electric layers can be observed in the sections. These include the topsoil layer with resistivity values ranging from $100 < \rho < 1000\Omega m$, the lateritic soil layer with resistivity values ranging from $500 < \rho < 3000\Omega m$, the fractured soil layer with resistivity values ranging from $3000 < \rho < 90000\Omega m$, and finally, the basement layer with resistivity values starting from $40\Omega m$ and extending to infinity. These distinct layers contribute to the overall characterization of the subsurface and provide valuable insights into the geological composition of the study area.

Iso-resistivity Map

The estimation of soil pipe extents was accomplished by mapping out the true resistivity values derived from the various geo-electric layers, in conjunction with the corresponding GPS coordinates obtained from the sites, as illustrated in Figures 7 and 8.

Based on the comprehensive analysis of the dipole-dipole survey results, the lithological models, and relevant literature sources such as Borah *et al*. (2022) [5], Gibson *et al*. (2004) [9], Got *et al*. (2020) [11], Joshi *et al*. (2021) [13], Li *et al*. (2015) [15], Mi *et al*. (2013) [17], it can be deduced that soil pipes tend to form in very close proximity to the surface. Consequently, for the purpose of mapping, the depth range considered extends from 0 to 5m.

Examining the maps, a notable feature is the anti-synclinal nature observed at the center, which represents the points of highest resistivity. Specifically, this can be observed in VES 5 and VES 2 for Awka site I, as well as VES 3 for Awka site II. These points serve as the inlet and outlet locations of

the soil pipes.

Furthermore, a careful examination of the maps provides insights into the potential migration paths of the soil pipes. For Awka site I and Awka site II, these paths align in a NE-SW direction, which coincides with the stress direction reported by Chibuogwu & Ugwu (2023a) [7] and the typical travel path of rainwater in the study areas. This observation leads to the inference that soil pipes are influenced by water flow paths that move from higher altitudes to lower altitudes, relying on the force of gravity. Consequently, they tend to form more readily in areas characterized by sloping terrain. This assertion finds support in previous studies conducted by Bhagyalekshmi *et al*. (2015) [4], Gilman & Newson (1980) [10], Onda (1994) [20], and Pierson (1983) [21].

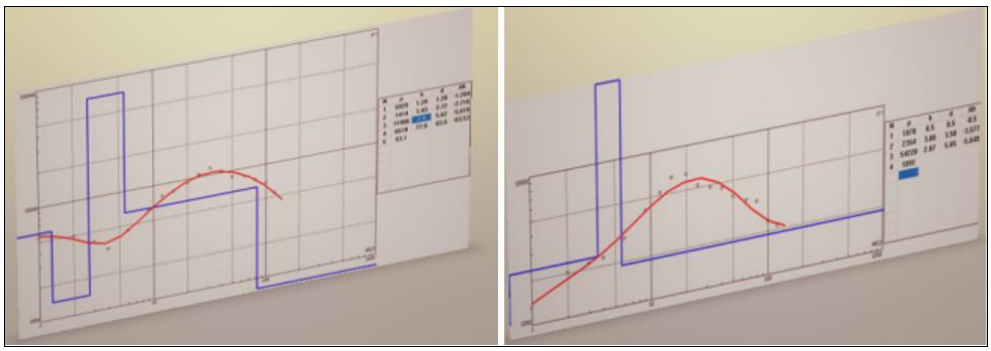

a)

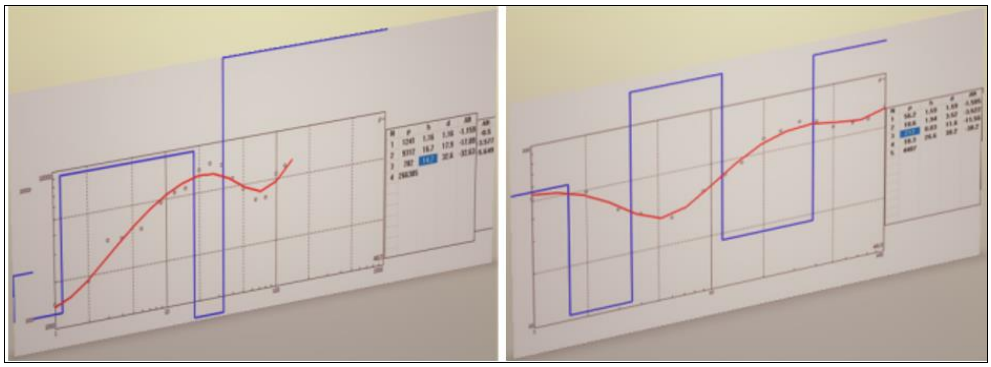

b)

**Fig 5:** Four representation of some of the VES curves for Awka site 1

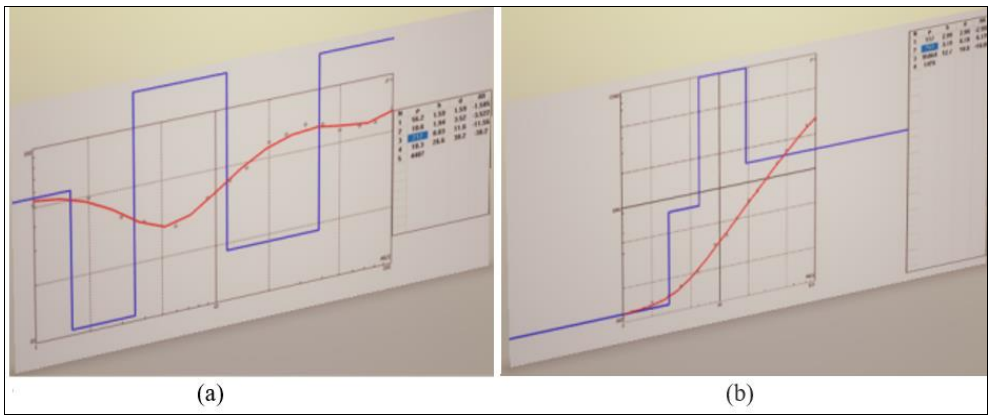

(a) (b)

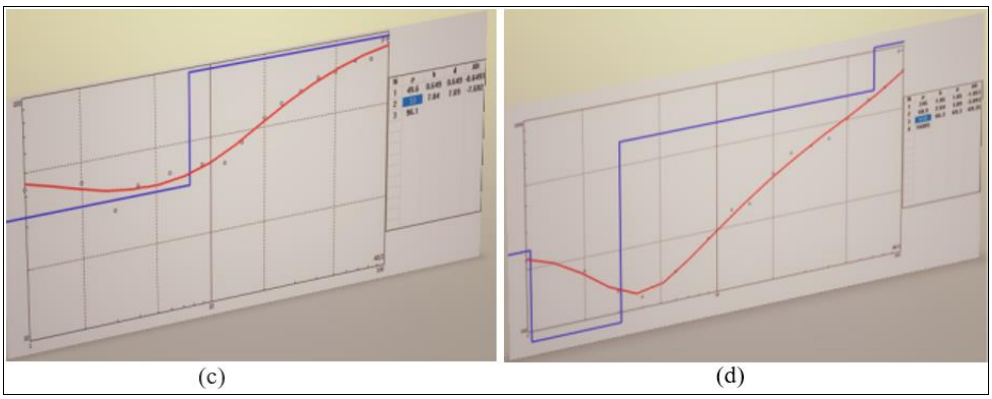

(c) (d)

**Fig 6:** Four representation of some of the VES curves for Awka site 2

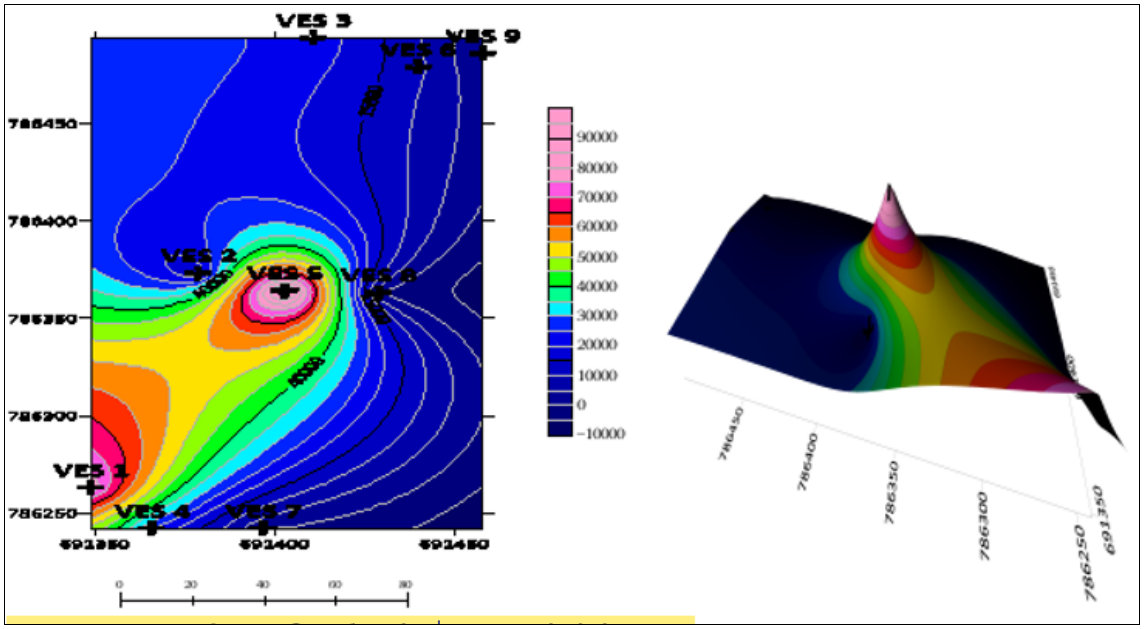


**Fig 7:** 2D and 3D of Awka site 1 Iso-resistivity map

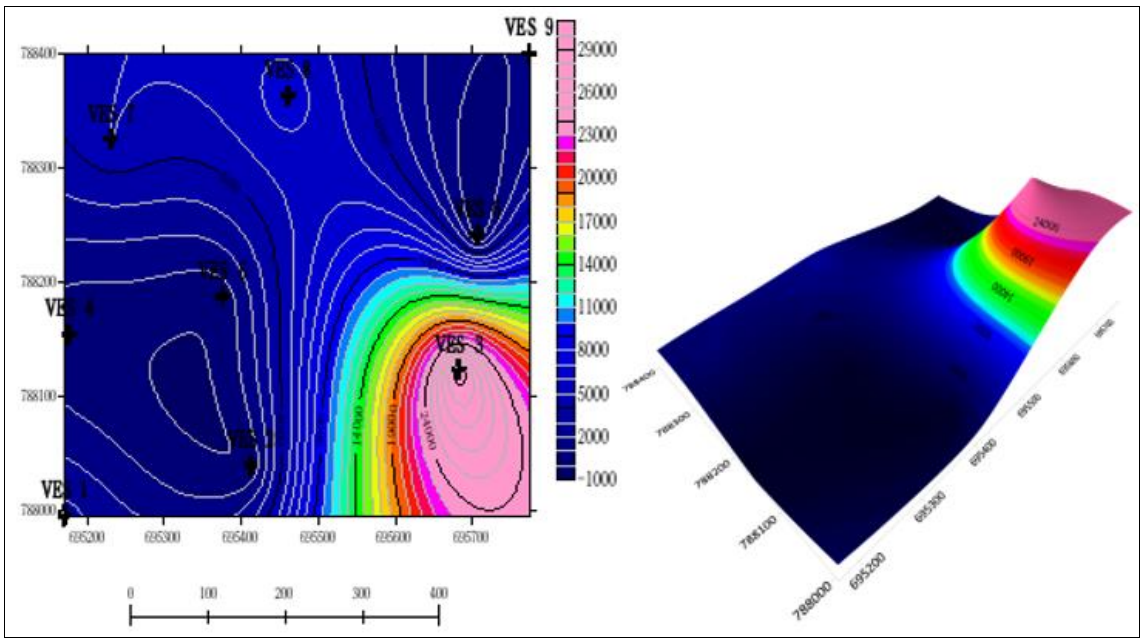


**Fig 8:** 2D and 3D of Awka site 2 Iso-resistivity map

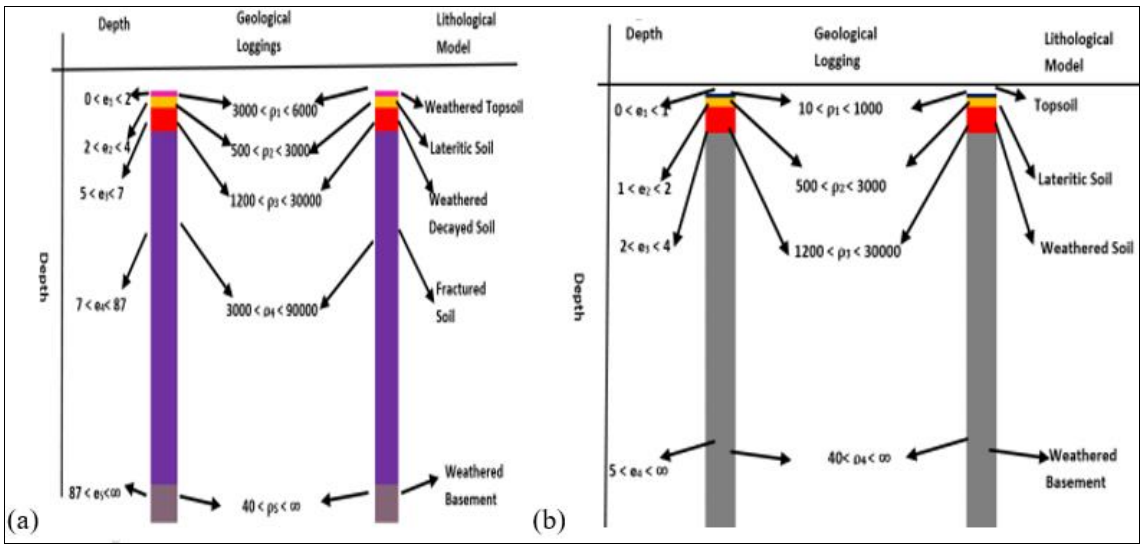

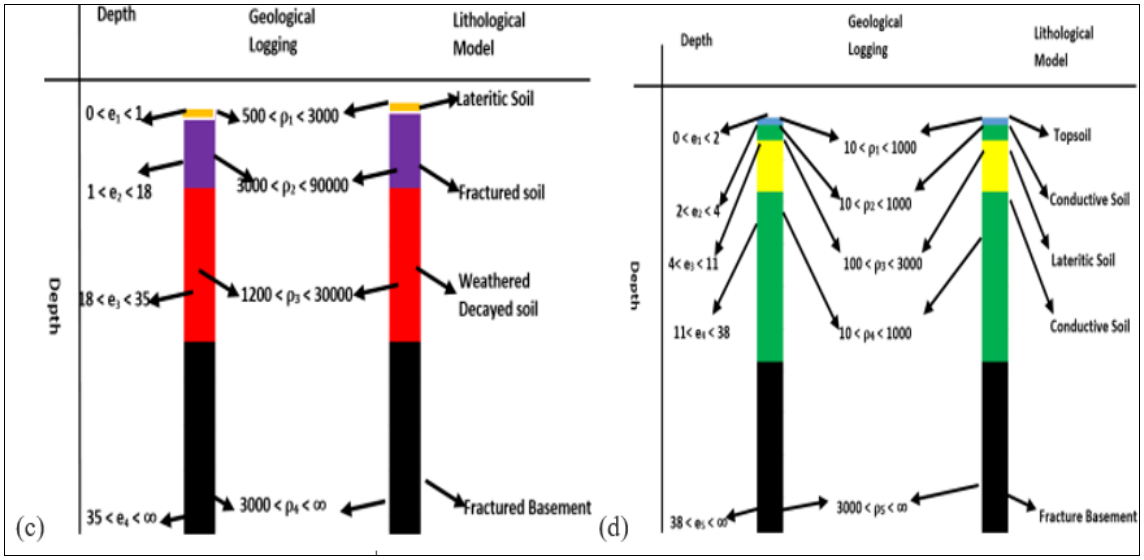


**Fig 9:** Four representation of Awka site 1 nine Geo-electric section

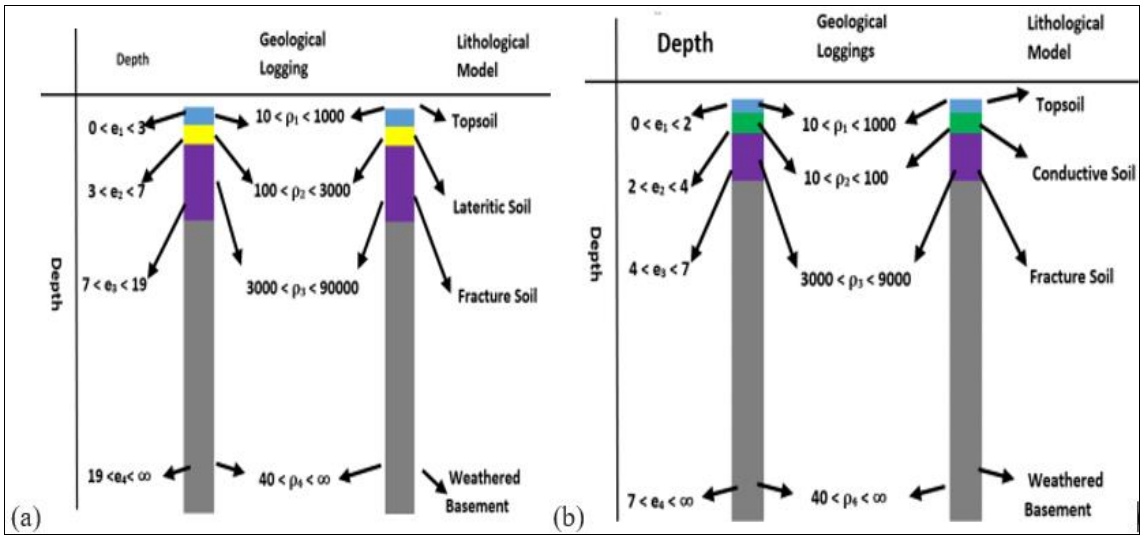


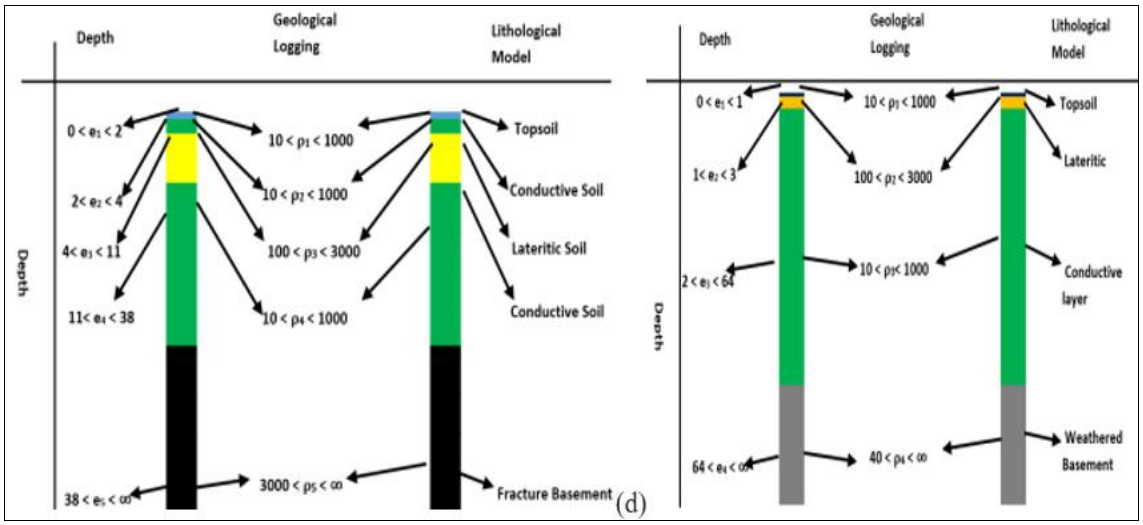


**Fig 10:** Four representation of Awka site 2 nine Geo-electric section

**Table 1:** Summary of Awka site 1 VES result

| Ves | Lat (N) | Long. (E) | ρ(Ω) | ∑ρ <5 m | Depth (m) | Thickness (m) | Curves |
|---|---|---|---|---|---|---|---|
| 1 | 6.22272 | 7.08117 | 5229.0 | 78549.0 | 1.280 | 1.280 | |
| | | | 1414.0 | | 2.720 | 1.430 | HKQ |
| | | | 71906.0 | | 4.620 | 2.90 | |
| | | | 6510.0 | | 83.50 | 77.90 | |
| | | | 531.0 | | | | |
| 2 | 6.22297 | 7.08104 | 60.80 | 16122.70 | 0.50 | 0.50 | HKH |
| | | | 12.20 | | 0.920 | 0.420 | |
| | | | 16015.0 | | 1.230 | 0.3140 | |
| | | | 34.70 | | 3.280 | 2.040 | |
| | | | 18.210 | | | | |
| 3 | 6.22314 | 7.08184 | 2517.0 | 23132.0 | 0.50 | 0.50 | KHK |
| | | | 19064.0 | | 0.9110 | 0.4110 | |
| | | | 1551.0 | | 2.110 | 1.260 | |
| | | | 25146.0 | | 7.760 | 5.60 | |
| | | | 262.0 | | | | |
| 4 | 6.22380 | 7.08199 | 130.0 | 24460.90 | 0.50 | 0.50 | HK |
| | | | 22.90 | | 0.3870 | 0.8870 | |
| | | | 24308.0 | | 0.5780 | 1.470 | |
| | | | 2528.0 | | | | |
| 5 | 6.22306 | 7.08197 | 16248.0 | 97221.0 | 0.50 | 0.50 | KHK |
| | | | 80973.0 | | 1.390 | 0.8850 | |
| | | | 27151.0 | | 10.710 | 9.290 | |
| | | | 5117.0 | | 82.10 | 71.50 | |
| | | | 1284.0 | | | | |
| 6 | 6.22330 | 7.08180 | 2515.0 | 11254.0 | 0.8390 | 0.8390 | AKQ |
| | | | 8739.0 | | 4.320 | 3.480 | |
| | | | 37448.0 | | 8.850 | 4.530 | |
| | | | 7462.0 | | 84.0 | 75.20 | |
| | | | 179.0 | | | | |
| 7 | 6.22393 | 7.08106 | 3.040 | 16.3690 | 2.020 | 2.020 | KHA |
| | | | 12.70 | | 1.860 | 3.880 | |
| | | | 0.6290 | | 3.450 | 7.330 | |
| | | | 1.750 | | 69.20 | 76.60 | |
| | | | 164.0 | | | | |
| 8 | 6.22319 | 7.08193 | 56.20 | 66.80 | 1.590 | 1.590 | HKH |
| | | | 10.60 | | 3.520 | 1.940 | |
| | | | 212.0 | | 11.60 | 8.040 | |
| | | | 18.30 | | 38.20 | 26.40 | |
| | | | 4407.0 | | | | |
| 9 | 6.22947 | 7.08178 | 24.50 | 30.590 | 1.050 | 1.050 | HA |
| | | | 6.090 | | 3.090 | 2.040 | |
| | | | 650.0 | | 69.30 | 66.30 | |
| | | | 1605.0 | | | | |
| 10 | 6. 23714 | 7.08224 | 1078.0 | 3432.0 | 0.50 | 0.50 | AK |
| | | | 2354.0 | | 3.580 | 3.080 | |
| | | | 54228.0 | | 5.650 | 2.070 | |
| | | | 1891.0 | | | | |
| 11 | 6.23673 | 7.08229 | 117.0 | 117.0 | 2.990 | 2.990 | AK |
| | | | 763.0 | | 6.180 | 3.190 | |
| | | | 95054.0 | | 18.80 | 12.70 | |
| | | | 1479.0 | | | | |
| 12 | 6.23629 | 7.08238 | 47.50 | 29898.50 | 1.580 | 1.580 | AK |
| | | | 146.0 | | 1.830 | 3.410 | |
| | | | 29705.0 | | 2.760 | 6.610 | |
| | | | 70.50 | | | | |
| 13 | 6.2372 | 7.08249 | 49.60 | 49.60 | 0.6490 | 0.6490 | H |
| | | | 33.0 | | 7.690 | 7.140 | |
| | | | 96.10 | | | | |
| 14 | 6.23672 | 7.08301 | 347.0 | 356.470 | 1.370 | 1.370 | HK |
| | | | 9.470 | | 1.680 | 0.3060 | |
| | | | 31594.0 | | 6.750 | 5.070 | |
| | | | 96.80 | | | | |
| 15 | 6.23622 | 7.08304 | 250.0 | 316.80 | 0.7090 | 0.7090 | K |
| | | | 66.80 | | 2.240 | 2.240 | |
| | | | 45.360 | | | | |
| 16 | 6.23725 | 7.08312 | 4020.0 | 5014.0 | 0.6650 | 0.6650 | HK |
| | | | 994.0 | | 1.610 | 0.9430 | |

| | | | | | | | |
|---|---|---|---|---|---|---|---|
| | | | 59961.0 | | 9.180 | 7.50 | |
| | | | 1931.0 | | | | |
| | 6.23671 | 7.08313 | 2355.0 | 2355.0 | 0.6920 | 0.6920 | HA |
| 17 | | | 14219.0 | | 17.50 | 16.80 | |
| | | | 1522.0 | | 34.80 | 17.30 | |
| | | | 31814.0 | | | | |
| | 6.23620 | 7.08325 | 1241.0 | 1241.0 | 1.160 | 1.160 | KA |
| 18 | | | 9312.0 | | 16.70 | 17.90 | |
| | | | 782.0 | | 14.70 | 32.60 | |
| | | | 266305 | | | | |

Magnetic Campaign

Figures 5 and 6 show the diurnal corrected results from the study areas. The diurnal-corrected data were obtained after the diurnal readings were removed from the magnetic field data obtained in the study areas. The magnetic data were obtained using a grid method of different cells. Individual cells from the grid assumed in the field show different anomalies, which were combined together using the kriging method to produce a surface map as shown in figures 5 and 6. The combined anomalies delineated different magnetic susceptibility contrasts among the rock types in the subsurface.

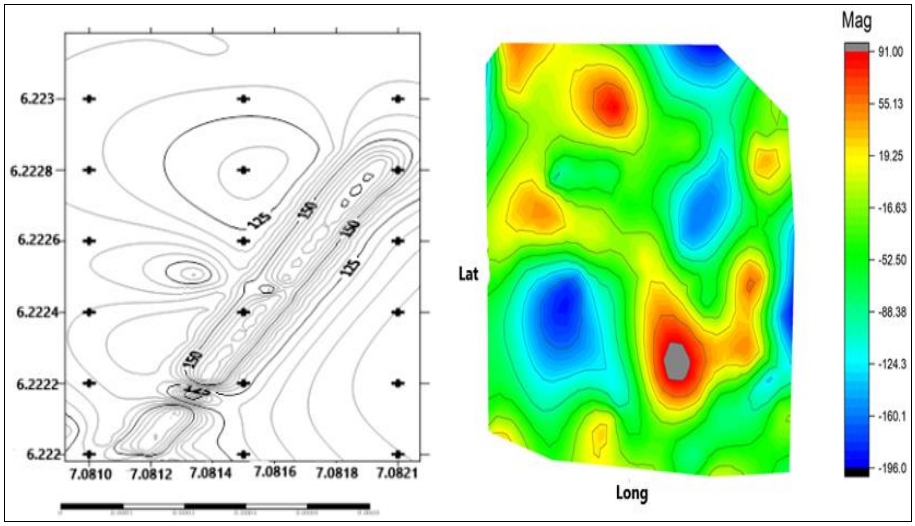


**Fig 11:** Contour map of Elevation and 2d magnetic diurnal corrected surface map for Awka site 1

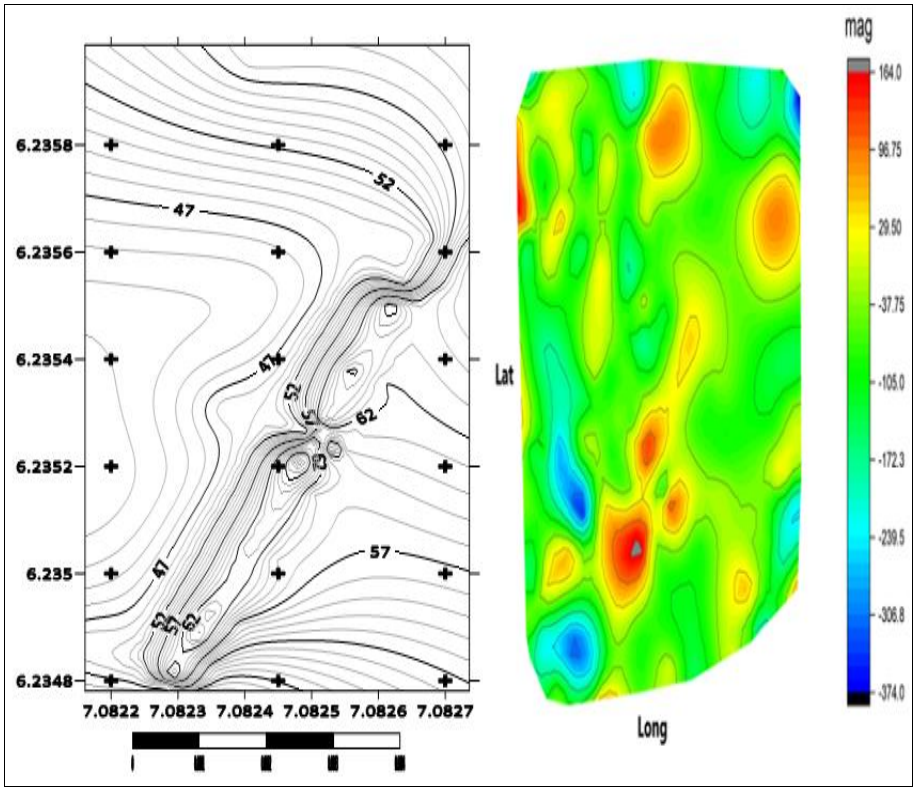


**Fig 12:** Contour map of Elevation and 2d magnetic diurnal corrected surface map for Awka site 2

The anomalies were observed to be in the range of <19.25nT (High magnetic anomaly) and >19.25 (low magnetic anomaly). Extreme magnetic high anomaly features, interpreted as a signature of inter-bedded/undisturbed sandstone/mudstone and/or highly magnetized shallow intrusion beneath the sediment, are of the range 40nT to 91nT predominately in the Northwestern zone and at the center part of Awka site 1. While in Awka site 2, they range from 30nT to 164nT and are predominantly in the northeastern region and southern part of the survey area. They are represented in yellow, red, and ash colours for the two study areas. The magnetic lows, ranging from -124.3nT to -200nT and -240nT to 300nT for both surveyed areas, are highlighted as light blue to dark blue in the geological interface (M. B. Rogers *et al*., 2005) [16]. The magnetic lows predominate in the western region of both survey areas. They are interpreted as sedimentary materials (clay and sand) that have been transported, drained, or dispersed by the action of running water (Kayode *et al*., 2014; Muhammad *et al*., 2014; Samuel *et al*., 2018) [14, 18, 23].

## Conclusions

In this study, our objective was to explore and interpret the spatial distribution of soil pipes in the Awka South Local Government Area of Anambra State, Nigeria, by employing two geophysical methods that were relatively unfamiliar in this context: the vertical electrical sounding (VES) technique and the magnetic technique.

To provide an overview of the VES results obtained along the dipole-dipole profiles, we presented various representations, including sounding curves, geoelectric sections, and iso-resistivity maps. The sounding curves offer insights into the changes in resistivity with depth, resulting in the generation of 14 curves (H, K, KA, HA, HK, AK, HKQ, HKH, KHK, AKQ, and KHA), which are contingent upon the electrical characteristics of the subsurface.

The abnormal resistivity distributions observed at depths of 35m and 85m, coupled with the vertical variations in the subsurface, led to the delineation of seven geo-electrical sections. These sections divide the subsurface into distinct regions that either promote or inhibit soil piping. The presence of fractured or weathered layers, as well as conductive layers, play a significant role in defining these areas.

Furthermore, the application of 3D iso-resistivity mapping enabled a more comprehensive description of the patterns and pathways of subsurface soil piping. This mapping revealed that soil piping tends to align with areas of structural stress, fluid migration patterns in the subsurface, and sloping terrains. Through these findings, we have established the effectiveness of the DC technique in detecting and studying the complex behaviors of soil piping in the subsurface.

Overall, this study demonstrates the successful utilization of the VES technique and the magnetic technique to investigate the phenomenon of tunnel erosion and gain valuable insights into the intricate nature of soil piping in the study area. The case study has also shown that the magnetic technique may be used to identify the position of soil pipes with low magnetic susceptibility. The result of the diurnal corrected anomaly generated from the field shows that low magnetic susceptibilities ranging from -124.4 to -300nT (Taking the range of the two study areas) are predominantly in the south western region of the surveyed areas, which perfectly coincides with the soil pipes located at the surface of the study area. However, further studies could be carried out in other places with different soil types to confirm the claim.

## Conflicts of Interest

There are no conflicts of interest among the authors

## References


1. Agagu OK, Adighije CI. Tectonic and sedimentation framework of the lower Benue Trough, southeastern Nigeria. Journal of African Earth Sciences. 1983;1(3-4):267-274. https://doi.org/10.1016/S0731-7247(83)80011-1
2. Atallah N, Shakoor A, Watts CF. Investigating the potential and mechanism of soil piping causing water-level drops in Mountain Lake, Giles County, Virginia. Engineering Geology. 2015;195:282-291. https://doi.org/10.1016/j.enggeo.2015.06.001
3. Bernatek-Jakiel A, Poesen J. Subsurface erosion by soil piping: Significance and research needs. Earth-Science Reviews. 2018;185:1107-1128. https://doi.org/10.1016/j.earscirev.2018.08.006
4. Bhagyalekshmi S, Mohan M, Sreedharan K, Ajaykumar B. Evaluation of the factors controlling the spatial distribution of soil piping: A case study from the southern Western Ghats, India. Arabian Journal of Geosciences. 2015;8(10):8055-8067. https://doi.org/10.1007/s12517-015-1793-8
5. Borah UK, Gond A, Rajan PP, Sivan R, Vivekanandan N. Joint geomorphological and geophysical (electrical resistivity) investigation for the configuration of soil pipe. Contributions to Geophysics and Geodesy. 2022;52(2). https://doi.org/10.31577/congeo.2022.52.2.4
6. Bryan RB. Soil erodibility and processes of water erosion on hillslope. Geomorphology. 2000;32(3-4):385-415. https://doi.org/10.1016/S0169-555X(99)00105-1
7. Chibuogwu IU, Ugwu GZ. An Open Investigation of Some Soil Pipes Forming Soil Subsidence at Awka South Local Government Area Using Very Low Frequency Electromagnetic Geophysical Technique. International Journal of Scientific Research in Multidisciplinary Studies. 2023a;9(2):40-45.
8. Chibuogwu IU, Ugwu GZ. Uncovering soil piping vulnerability using direct current geophysical techniques in Awka, Anambra State, Nigeria. International Journal of Multidisciplinary Research and Growth Evaluation. 2023b;4(3):426-450. https://doi.org/10.54660/.IJMRGE.2023.4.3.426-450
9. Gibson PJ, Lyle P, George DM. Application of Resistivity and Magnetometry 1 Geophysical Techniques for Near-Surface Investigations in Karstic Terrains in Ireland. Journal of Cave 2 and Karst Studies. 2004;66:35-38.
10. Gilman K, Newson MD. Soil Pipes and Pipeflow A Hydrological Study in Upland Wales. Geo Abstract; c1980. p. 100.
11. Got J-B, Bielders CL, Lambot S. Characterizing soil piping networks in loess-derived soils using ground-penetrating radar. Vadose Zone Journal. 2020;19(1). https://doi.org/10.1002/vzj2.20006

12. Gouet DH, Meying A, Ekoro Nkoungou HL, Assembe SP, Njandjock Nouck P, Ndougsa Mbarga T. Typology of Sounding Curves and Lithological 1D Models of Mineral Prospecting and Groundwater Survey within Crystalline Basement Rocks in the East of Cameroon (Central Africa) Using Electrical Resistivity Method and Koefoed Computation Method. International Journal of Geophysics; c2020. p. 1-23. https://doi.org/10.1155/2020/8630406
13. Joshi M, Prasobh PR, Rajappan S, Rao BP, Gond A, Misra A, *et al*. Detection of soil pipes through remote sensing and electrical resistivity method: Insight from southern Western Ghats, India. Quaternary International; c2021. p. 575-576, 51-61. https://doi.org/10.1016/j.quaint.2020.08.021
14. Kayode JS, Nyabese P, Adelusi AO. Ground magnetic study of Ilesa east, Southwestern Nigeria. African Journal of Environmental Science and Technology. 2014;4(3):122-131.
15. Li S, Liu B, Nie L, Liu Z, Tian M, Wang S, *et al*. Detecting and monitoring of water inrush in tunnels and coal mines using direct current resistivity method: A review. Journal of Rock Mechanics and Geotechnical Engineering. 2015;7(4):469-478. https://doi.org/10.1016/j.jrmge.2015.06.004
16. Rogers MB, Cassidy JR, Dragila MI. Ground-based magnetic surveys as a new technique to locate subsurface drainage pipes: A case study. Applied Engineering in Agriculture. 2005;21(3):421-426. https://doi.org/10.13031/2013.18461
17. Mi KP, Samgyu P, Myeong-Jong Y, Changryol K, Jung-Sul S, Jung-Ho K, *et al*. Application of electrical resistivity tomography (ERT) technique to detect underground cavities in a karst area of South Korea. Environ Earth Sci. 2013;50(2):256-267.
18. Muhammad SB, Udensi EE, Momoh M, Sanusi YA, Suleiman T, Ajana O. Spectral Analysis and Estimation of Depths to Magnetic Rocks below the Katsina Area, Northern Nigerian Basement Complex. RRJoPHY. 2014;3:13-23.
19. Olafisoye ER. Groundwater Contaminats' Investigation at Aarada Waste Disposal Site Using Geophysical and Hydro-Physicochemical Approach. IOSR Journal of Environmental Science Toxicology and Food Technology. 2013;2(4). https://doi.org/10.9790/2402-0240110
20. Onda Y. Seepage erosion and its implication to the formation of amphitheatre valley heads: A case study at Obara, Japan. Earth Surface Processes and Landforms. 1994;19(7):627-640. https://doi.org/10.1002/esp.3290190704
21. Pierson TC. Soil pipes and slope stability. Quarterly Journal of Engineering Geology. 1983;16(1):1-11. https://doi.org/10.1144/GSL.QJEG.1983.016.01.01
22. Rayment RA. Aspects of the Geology of Nigeria. Ibadan University Press; c1965.
23. Samuel YM, Saad R, Muztaza NM, Saidin MM, Muhammad SB. Integration of Magnetic and Geotechnical methods for Shallow Subsurface Soil Characterization at Sungai Batu, Kedah, Malaysia. Journal of Physics: Conference Series. 2018;995:012090. https://doi.org/10.1088/1742-6596/995/1/012090
24. Wright JB. South Atlantic continental drift and the Benue Trough. Tectonophysics. 1968;6(4):301-310. https://doi.org/10.1016/0040-1951(68)90046-2
25. Zohdy A. Use of Dar Zarrouk curves in the interpretation of vertical electrical sounding data; c1974. https://doi.org/10.3133/b1313D